NATIONAL ADVISORY COMMITTEE FOR AERONAUTICS

TECHNICAL NOTE 2246

METHOD FOR DETERMINING DISTRIBUTION OF LUMINOUS EMITTERS IN CONE OF LAMINAR BUNSEN FLAME

By Thomas P. Clark

Lewis Flight Propulsion Laboratory
Cleveland, Ohio

Washington
January 1951

NATIONAL ADVISORY COMMITTEE FOR AERONAUTICS

TECHNICAL NOTE 2246

METHOD FOR DETERMINING DISTRIBUTION OF LUMINOUS EMITTERS IN CONE OF LAMINAR BUNSEN FLAME

By Thomas P. Clark

SUMMARY

A method is described for calculating the intensity distributions in the images of Bunsen burner cones having either uniform or non-uniform distributions of emitters in the luminous zones. A means is also presented for determining the distribution of the emitters in the luminous zone of a Bunsen cone from an analysis of the intensity distribution in the optical image of a given cone.

An intensity distribution in a Bunsen cone image resulting from the free radical C_2 radiation is analyzed as an example of the application of the method. The analyzed trace indicates that the C_2 emitter distribution in the luminous zone has a maximum near the center of the luminous zone. The shape of the C_2 emitter distribution curve remained the same for different fuel-air ratios, although the concentration of C_2 emitters markedly increased with the richer fuel-air mixtures. The thickness of the luminous zone due to C_2 radiation remained the same for various fuel-air ratios and was approximately 0.25 millimeter.

INTRODUCTION

Recent work in flame spectroscopy suggests the need for a method of determining the distribution throughout the reaction zone of the radiating diatomic molecules that generate a flame spectrum. Spectroscopic studies of flames (references 1 and 2) indicate that these emitters are not uniformly distributed in the luminous reaction zone. A method for determining the thickness of a Bunsen flame cone that may be adapted to the determination of the relative concentrations of emitters in different regions of the luminous reaction zone is described in reference 3. This method involves the mathematical analysis of the change in intensity of the image of a luminous cylindrical shell, viewed normal to its axis. The intensity distribution of the

emitter can be determined by analyzing the density distribution of the flame image in a photographic negative; the emitter concentration across the flame front can be calculated by use of the intensity-distribution data.

This investigation conducted at the NACA Lewis laboratory develops, in a simplified manner, the Hűbner-Klăukens equation for calculating the intensity distribution in the image of a luminous ring having the emitters uniformly distributed through the cross section and shows, in addition, how this equation can be used to calculate the intensity distribution in images of luminous rings having cross sections containing nonuniform distributions of emitters. The process of determining the cross-sectional emitter distribution of a luminous ring from an analysis of the intensity distribution in the optical image of the given ring is next developed. Finally, the limitations and the experimental requirements of the method and its application to flame cones are discussed.

INTENSITY DISTRIBUTION IN IMAGES OF LUMINOUS CONES

Cones with Uniform Distributions of Emitters in Cross Section

The luminous region of the inner cone of a Bunsen flame has a finite thickness. An equation to determine this thickness from an analysis of the intensity distribution in the image of a Bunsen cone is developed in reference 3. The study of the cross-sectional intensity of a luminous cone at a given radius normal to the axis of the cone is equivalent to the study of the cross-sectional intensity of a right cylinder of the same radius, and this simplification will be used in the present discussion (fig. 1). In the cylindrical model, the intensity at any point in the given cross section at a radius x from the center is the same. The intensity is also constant along a normal to the cross section at any point x; thus a cylindrical symmetry exists and a study of cross-sectional intensities can be limited to a single cross section.

The equations for intensity distribution are developed for an idealized optical system in which the lens is assumed to have infinite resolution, and the diaphragm aperture is infinitely small (fig. 2). This development allows the intensity distribution to be calculated in terms of the single ray $M_0M'_0$. When the ray passes through the origin A, the thickness of ring wall crossed is equal to 2 BC. As the ray sweeps toward the outer edge of the ring, the thickness of ring wall crossed is no longer measured parallel to a ray through the

origin A, and the increments of ring-wall thickness are increased in length by the secant of the turning angle θ. If a ten-times magnified image of a small flame cone is used in the analysis, the change in length is negligible. The thickness of ring wall passed through by the ray can therefore be calculated to an accuracy adequate for most experimental work by assuming that the ray $M_0M'_0$ does not pivot about point M'_0 but instead moves along the radius Ax and remains parallel to its position at the origin. All variations in wall thickness are measured parallel to each other in this instance and can be expressed by a simple algebraic equation.

The intensity distribution in the optical image of a luminous ring with a uniform distribution of emitters in the cross section is equivalent to the change in thickness of wall cut by line MM' as it moves from the center of the ring to the outer edge of the ring along a radius normal to the line (fig. 3).

An examination of figure 3 reveals that the portion of the ring below the x-axis is a mirror image of the portion above it. The ring-wall thickness above the x-axis can therefore be calculated and multiplied by 2 to give the total ring-wall thickness at any point. With reference to figure 3, the equation for ring-wall thickness at any point d can be derived in the following manner:

$$\frac{1}{2}S = y_o - y_i$$

$$y_o = \sqrt{r_o^2 - x^2}$$

$$y_i = \sqrt{r_i^2 - x^2}$$

therefore

$$S = 2\left(\sqrt{r_o^2 - x^2} - \sqrt{r_i^2 - x^2}\right) \qquad (1)$$

At the origin:

$$y_i = r_i$$

$$y_o = r_o$$

$$\frac{1}{2} S_0 = r_o - r_i$$

$$S_0 = 2(r_o - r_i)$$

$$S_{relative} = \frac{S}{S_0}$$

therefore

$$S_{relative} = \frac{\sqrt{r_o^2 - x^2} - \sqrt{r_i^2 - x^2}}{r_o - r_i} \qquad (2)$$

where

r_i any radius to inside edge of given ring

r_o any radius to outside edge of given ring

S any ring-wall thickness

S_0 ring-wall thickness along diameter

x any distance along x-axis

y_i radius of inner wall of cylinder

y_o radius of outer wall of cylinder

Inasmuch as relative ring-wall thickness is equivalent to intensity, equation (2) is the same as the expression developed in reference 3.

In figure 4 is shown a plot of ring thickness traversed by MM' on a ring of $r_o = 2.0$ millimeters and $(r_o - r_i) = 0.1$ millimeter. The plot in figure 4 has symmetrical axes. If the horizontal scale is expanded tenfold, the shape of the important end portion of the curve is more easily seen (fig. 5). This expanded horizontal scale will be used in all subsequent plots.

Cones with Nonuniform Distributions of Emitters in Cross Section

If the wall of the luminous cylinder is treated as if it were constructed of concentric shells of wall thickness ds, the cross section of the cylinder can be represented as shown in figure 6. Each r_o would become r_n and each r_i would become r_{n-1}. Each ring of outer radius r_n and inner radius r_{n-1} can be treated by means of equation (2). The lengths of path traversed in each incremental ring by the ray MM' passing through a given point d can be summed from $r = r_i$ to $r = r_o$, giving the same result as equation (2); namely,

$$S_{relative} = \frac{\sum_{r_i}^{r_o} \left(\sqrt{r_n^2 - x^2} - \sqrt{r_{n-1}^2 - x^2} \right)}{\sum_{r_i}^{r_o} (r_n - r_{n-1})}$$

In order to determine the intensity along ray MM' passing through d, each ring intercept of the ray MM' through d must be multiplied by the number of emitters per centimeter and then the individual resultant intensities from r_i to r_o along the ray MM' must be added. Inasmuch as the emitters are equally spaced on the line MM' for a cross section having a uniform distribution of emitters, the problem can be simplified in this case to the point represented by equation (2).

For the case of the cross section having a variable distribution of emitters, however, these simplifications cannot be used. The complete process of multiplying each ring intercept by its appropriate intensity step along a ray and summing the resultant intensity increments must be carried out.

This method of calculation requires that each individual ring increment have a uniform cross-sectional emitter distribution; that is, the top of the graphical representation of the distribution for each ring segment should be flat, as shown in figure 7(a). The representation of the cross-sectional distribution will then no longer be a smooth curve, but will be a chord plot, as shown in figure 7(b) for a straight-line distribution. In the subsequent figures, a smooth curve has been drawn through the chords, as shown in figure 7(b).

With only 10 rings, some discrepancy may exist between the actual image intensity distribution and that calculated by means of the chord-plot cross-sectional distribution. The magnitude of the difference will be dependent on the steepness of the cross-sectional concentration gradient and the amount of curvature in the distribution curve. This chord-plot distribution is adequate, however, for distinguishing the types of image intensity distribution resulting from various emitter distributions. Each of figures 7(a) to 7(g) is a plot of intensity distribution in images of luminous rings with the same central intensity when the distribution of emitters in the cross section is as shown by the dashed curve in the figure and of the form indicated by the equations noted.

ANALYSIS OF LUMINOUS CONE IMAGES

The emitter distribution in the luminous ring is determined by solving a series of n simultaneous equations for the intensity distribution lying along a series of n rays from r_o to r_i. The equations are based on figure 8 as follows:

$$A_1 a = I_1$$

$$A_2 a + B_2 b = I_2$$

$$A_3 a + B_3 b + C_3 c = I_3$$

$$\vdots \quad \vdots \quad \vdots$$

$$A_{10} a + B_{10} b + C_{10} c + D_{10} d + E_{10} e + F_{10} f + G_{10} g + H_{10} h + J_{10} j + K_{10} k = I_{10}$$

The values of A to K are the geometric intercepts of the concentric rings, and the subscripts indicate the position on the x-axis that the rays pass through. The I-values are the intensity values for the rays indicated by the subscript. The average relative emitter concentrations for the ring segments are designated a to k. If the values of these small letters are plotted against the corresponding intensity-distribution abscissae, a chord plot of the relative concentration of emitters across the luminous zone results.

REQUIREMENTS OF METHOD

In order for the method to be adequate, the following experimental requirements must be met:

1. The flame cone of a hydrocarbon and air mixture burning at atmospheric pressure has a wall thickness of approximately 0.2 millimeter. For optimum results it should not move laterally during an exposure more than ±1.0 percent of this value, although with a 10-ring analysis as much as ±5.0 percent lateral motion may be tolerated.

2. The fuel-air ratio should be held constant during the exposure. The use of premixed gaseous fuel and air at low flow rates allows this requirement to be met with an error of not over 1.0 percent.

3. The image of the flame to be photographed must come from only one emitter. In figure 9 are shown the locations of the bands of a flame spectrum and the transmission characteristics of filters that can be used to isolate the radiation from each of the three luminous emitters responsible for flame spectra. No single filter was found that would completely isolate the free radical CH spectrum; however, using a Wratten No. 1 filter in combination with a Corning CG-G-985-B filter, as indicated, isolates the CH radiation except for a weak C_2 band at 4381 A. This weak radiation should not register during an exposure for CH radiation.

4. The details of the flame cross section must be resolved. As previously mentioned, the bright edge of the flame is approximately 0.2 millimeter wide, and this width must be divided into from 10 to 100 parts to be analyzed. A magnified image would seem to be the most logical approach, but magnification is accompanied by a rapid decrease in the depth of field in sharp focus. A balance between magnification, resolution, and depth of field must be determined to obtain optimum results. Spectrographic plates will resolve approximately 60 lines, or 120 increments per millimeter; thus negative material is not a limiting factor. Calculations show that using a magnification of 10 diameters, a radiation wavelength of 4000 A, and a photographic aperture of f/4.5, approximately 80 lines or 160 increments can be resolved in 0.2 millimeter of image. It should be possible, in practice, to distinguish 100 increments in the 0.2-millimeter flame zone by allowing a margin of error for departure from theoretically perfect optics.

5. The densitometer used to measure the image densities must resolve the details of the image in the negative. This requirement

is not difficult to obtain inasmuch as recording microphotometers commonly use a slit width of 0.01 millimeter, which would give a 0.5-percent accuracy on a 0.2-millimeter flame edge magnified 10 times.

6. Image intensity values must be obtained from the values of density in the photographic image. These values can be acquired by including a series of graded intensity exposures on each photographic plate. A calibration curve can be made from the intensity against density values of the series of graded exposure steps. The intensities in the flame image can then be read directly from the calibration curve.

LIMITATIONS OF METHOD

This analytical method is subject to several limitations that must be considered in its utilization. It is suitable only for rigid flames of premixed gaseous fuel and oxidant. The flame must be fed by a constant-pressure, constant-composition combustible supply. The flame must have cylindrical symmetry. The resolution of the image of the flame zone is limited by the theoretical optics of the photographic system, as described in the preceding section. Although many reaction products are postulated in the combustion reaction, only the OH, CH, and C_2 free radicals are known to radiate in the wavelength region available to photographic emulsions (reference 4). The photography of the free radical OH radiation offers additional difficulties because it lies beyond the wavelength range of glass optics. In addition, the analysis of its intensity pattern is complicated by the presence of OH free radicals in both the inner and outer cones and by the absorption of radiation by the OH free radicals. The radiating free radicals of each of these species represent only a fraction of the total number of these species present in the reaction zone. No simple method exists for determining this ratio, especially under nonequilibrium conditions.

In spite of these limitations, however, data of sufficient accuracy to permit the determination of the general nature of the distribution of the emitters of each type throughout the reaction zone should be obtainable. Also, comparison of the relative changes in concentration of the emitter throughout the reaction zone for changes in fuel-oxidant ratio should be possible.

EXPERIMENTAL PROCEDURE

A commercial fuel gas, which consists largely of propane, was burned with air as a Bunsen cone on a pyrex tube 100 centimeters long

with an internal diameter of 0.6 centimeter. A photograph of the flame was made by means of a microtessar lens. The object and image distances were adjusted to focus a tenfold magnified image of the flame onto the photographic plate. Eastman III-F spectroscopic plates were used as negative material. A Wratten No. 4 filter was placed between the lens and the film to isolate the C_2 radiation. Trial exposures were made at three different fuel-air ratios until exposure times had been determined that gave the same central intensity in the flame images for each fuel-air ratio.

The photographic plate was covered with a black paper sheet having a small square hole near one edge. The image of the flame was focused on this hole and a series of exposures of increasing duration was made. After each exposure the plate was moved so as to expose a fresh portion of it. When the series of exposures had been completed, the paper mask was removed and a narrow strip of black paper was fastened over the exposed area. A final exposure of the whole flame was then made on the uncovered portion of the plate. This procedure was repeated for three fuel-air ratios, each photographed with lens apertures of f/4.5, f/8, and f/16. The plates were developed for 4 minutes at 20° C in D-19 developer. The plates were stroked continuously with a cotton swab during development to insure uniform development of the images.

Each processed plate was mounted in a recording microdensitometer and a trace was made of the exposure steps, the central flame density, and the flame edge at a Bunsen cone diameter of 4 millimeters (4.0 cm in the magnified image). The exposure steps were utilized to transform film density to image intensity. The ordinate value of each trace was divided by the ordinate value of its central intensity. This division normalized the results and facilitated comparison of the curves. These curves were then analyzed for the emitter distribution, as described earlier in the report.

RESULTS

The initial experimentation on exposure times revealed that the intensity of the C_2 radiation from the flame varied markedly with fuel-air ratio. Lean flames required several times more exposure than did rich flames to register the same central image density on the photographic plate. When several traces from flames of each different fuel-air ratio were normalized and compared, the shapes of the flame traces were the same within the limits of experimental error. This likeness suggests that the thickness of the luminous reaction zone

remains the same for different fuel-air ratios. In addition, the shape of the distribution curve apparently remains the same, although the concentrations are higher in richer flames. Variations in lens aperture had no apparent effect on the shape of the flame trace.

Inasmuch as neither changes in fuel-air ratio nor changes in lens aperture affected the shape of the density trace, one characteristic trace was selected for analysis. The density trace was replotted as an intensity trace with the aid of the calibration curve from the intensity-against-density step wedge included on the photographic negative. The resulting intensity trace is shown by the solid-line curve on figure 10. This curve and equation (2) were used to calculate the emitter distribution for C_2. The calculated emitter distribution is shown by the dashed-line curve on figure 10. The absolute concentrations of C_2 emitters in flames have been determined (reference 5), and these data were utilized to calculate the absolute concentrations of C_2 emitters throughout the reaction zone. For this purpose, it was assumed that the effect of nitrogen on the concentration of C_2 emitters was the same for propane as it was for acetylene and ethane in reference 5. The calculated concentrations are given by the far left ordinate in figure 10. The shape of the distribution curve is consistent with prevailing theories of hydrocarbon combustion. The rapid initial increase of the C_2 concentration is in line with the rapid temperature increase postulated for the combustion reaction. The emitter concentration reaches a maximum near the center of the reaction zone and then decays at a somewhat slower rate than the rate of the initial concentration increase.

DISCUSSION

A low-power microscope was used to determine whether flame motion was present. The tip of the flame exhibited a slight flicker. The maximum displacement of the luminous zone at this point was equivalent to approximately twice the thickness of the luminous zone. The flame diameter of 4.0 millimeters, which was used in the analysis, occurred at one-third of the distance from the base to the tip of the flame. When the flame was examined at this point, well down on the flame cone, no lateral flame-front motion was apparent. With the flame assumed to be a right cone, calculation of the possible effect of the tip flicker on the lateral motion of the flame at the 4.0-millimeter diameter indicated that the effect would be negligible. On the basis of the previously mentioned optical resolution, the position of an intensity value can be located in a reaction zone 0.2 millimeter thick with an error under 1.0 percent.

The analytical method was based on the assumption that the photographic aperture was infinitely small. The effect of a finite photographic aperture on the intensity distribution in the image was calculated in reference 3 and found to be negligible. The principal error in the analysis would thus seem to be the error introduced by the use of a finite number of steps in the numerical integration. Check calculations based on 100 increments in the reaction zone were made for the straight-line distributions shown in figures 7(b) and 7(d). In figure 7(b), the analysis was in error by 30 percent at $x = 1.99$. The error dropped rapidly to substantially less than 5 percent at $x = 1.90$. The errors in figure 7(d) were all less than 5 percent.

Inasmuch as there were no discrete particles to be resolved in the flame image, resolving power and the lack of sharpness in elements out of the plane of focus were insignificant factors in determining image intensity. Out-of-focus elements of the light flux in the luminous zone probably overlapped each other in the flame image. This overlapping would tend to bring the local intensity back to its original value by integrating the intensity of several weak, enlarged, and superimposed out-of-focus images.

Inasmuch as the detailed mechanism of combustion is unknown, the reason for the decay of the C_2 radiation cannot be definitely stated. The lack of exact knowledge regarding the temperature distribution in the reaction zone further complicates any attempted analysis. The radiating molecules are, in all probability deactivated by collision, but whether collisions and deactivation are accompanied by reaction with oxygen or by polymerization to form smoke cannot be determined on the basis of known data. The calculation of the emitter distribution also determines the thickness of the luminous reaction zone. The C_2 distribution calculation has shown the luminous reaction zone to be approximately 0.25 millimeter thick.

CONCLUDING REMARKS

The experimental work with the free radical C_2 emitter indicates that the analytical method proposed can be successfully applied to the analysis of the emitter concentrations in the reaction zone of a Bunsen flame. Inasmuch as it was found (1) that Bunsen flames could be successfully stabilized, and (2) that within reasonable limits the depth of field in focus did not alter the image intensity pattern, the precision of locating a given intensity in the luminous reaction

zone is limited only by the resolving power of the photographic objective. Under optimum conditions, the position of an intensity value can therefore be located in a reaction zone 0.2 millimeter thick with an error under 1.0 percent.

The method should be applicable to the analysis of intensity and concentration distributions of emitters other than C_2, such as the free radicals OH, CH, and CO. It might also be applied to emitters from luminous reactions involving fuels other than hydrocarbons and oxidants other than air.

Lewis Flight Propulsion Laboratory,
National Advisory Committee for Aeronautics,
Cleveland, Ohio, August 23, 1950.

REFERENCES

1. Gaydon, A. G., and Wolfhard, H. G.: Spectroscopic Studies of Low-Pressure Flames. Third Symposium on Combustion and Flame and Explosion Phenomena, The Williams & Wilkins Co. (Baltimore), 1949, pp. 504-518.

2. Wolfhard, H. G., and Parker, W. G.: Combustion Processes in Flames. Part VI. A New Technique for the Spectroscopic Examination of Flames at Normal Pressures. Rep. No. CHEM.457, British R.A.E. March 1949.

3. Hübner, H.-J., und Kläukens, H.: Berechnung der Intensitätsverteilung im Bilde eines Flammenkegels. Ann. Phys., Folge 5, Bd. 39, 1941, S. 33-50.

4. Gaydon, A. G.: Spectroscopy and Combustion Theory. Chapman and Hall, Ltd. (London), 2d ed., 1948, pp. 38-39.

5. Gaydon, A. G., and Wolfhard, H. G.: Spectroscopic Studies of Low-Pressure Flames. IV. Measurements of Light Yield for C_2 Bands. Proc. Roy. Soc., vol. 201, no. 1067, ser. A, May 1950, pp. 570-585.

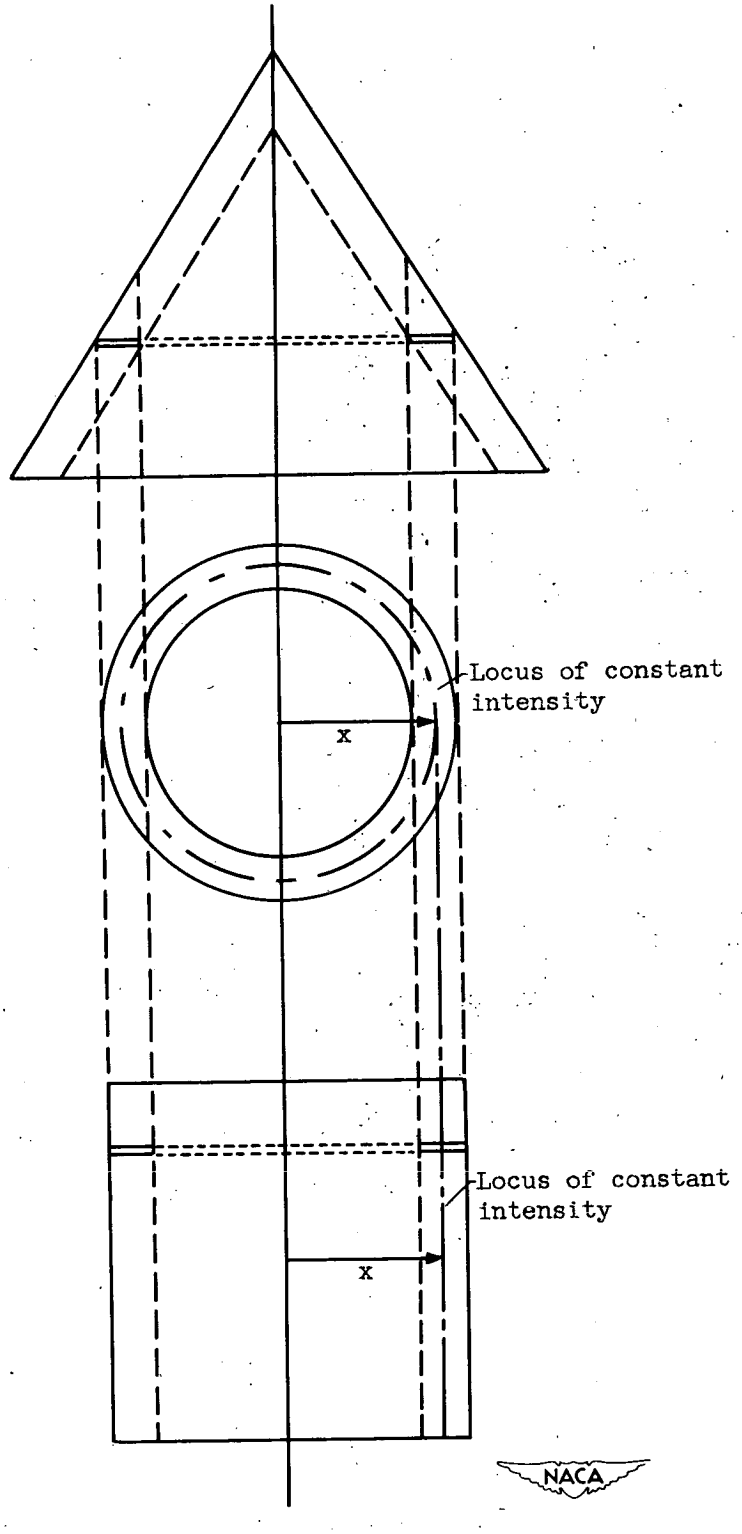

Figure 1. - Geometric model of flame cone as compared with right cylinder of equivalent cross section.

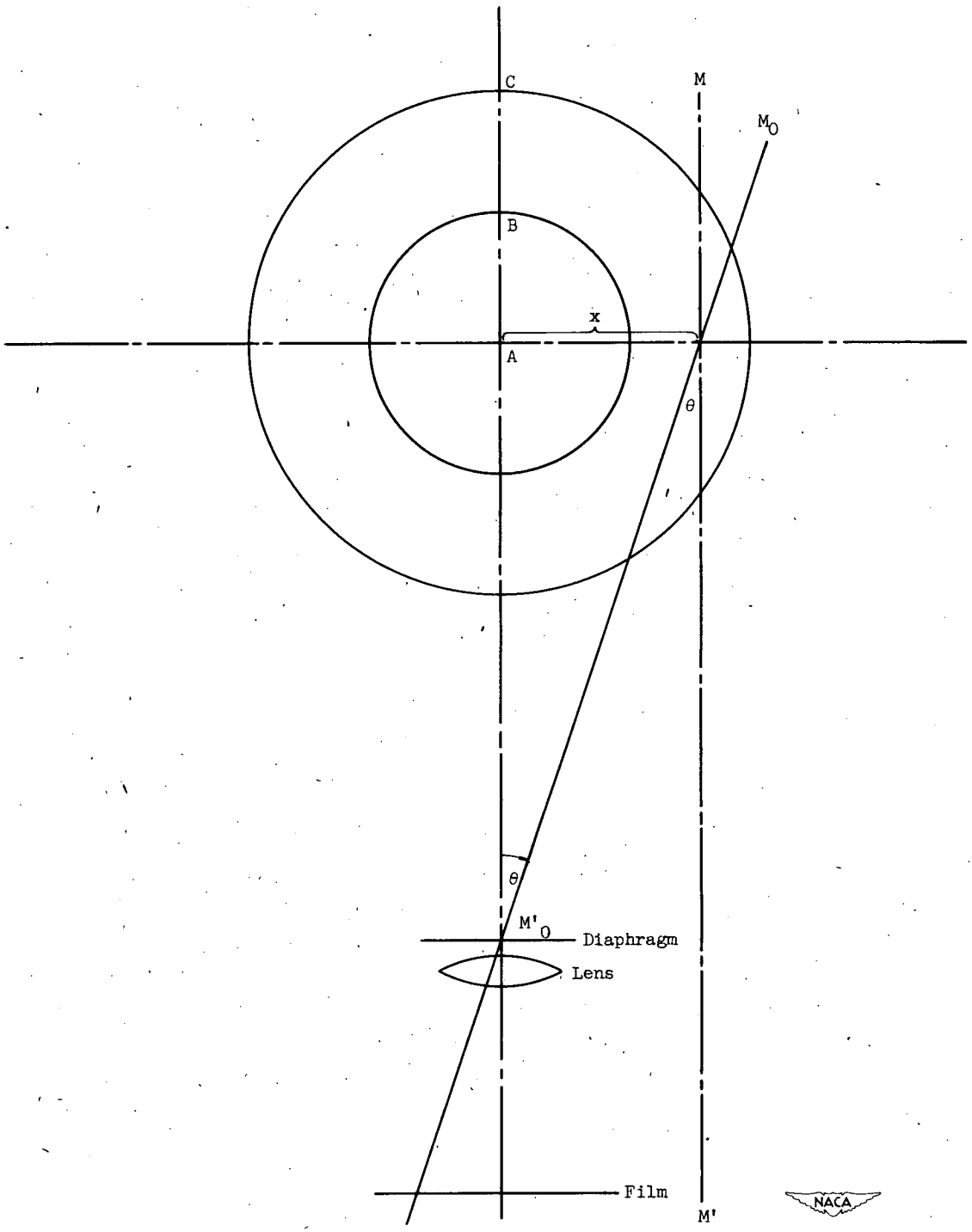

Figure 2. - Geometric model for analysis of luminous ring.

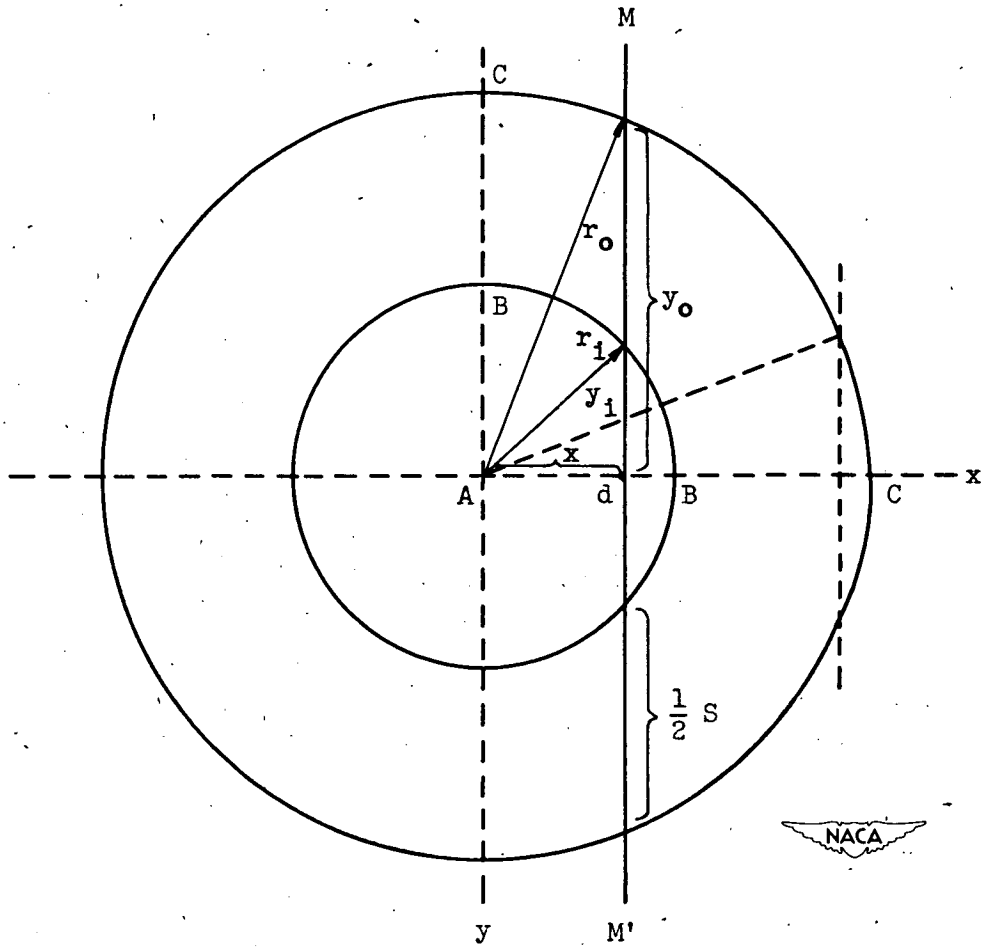

Figure 3. - Method of calculating ring thickness.

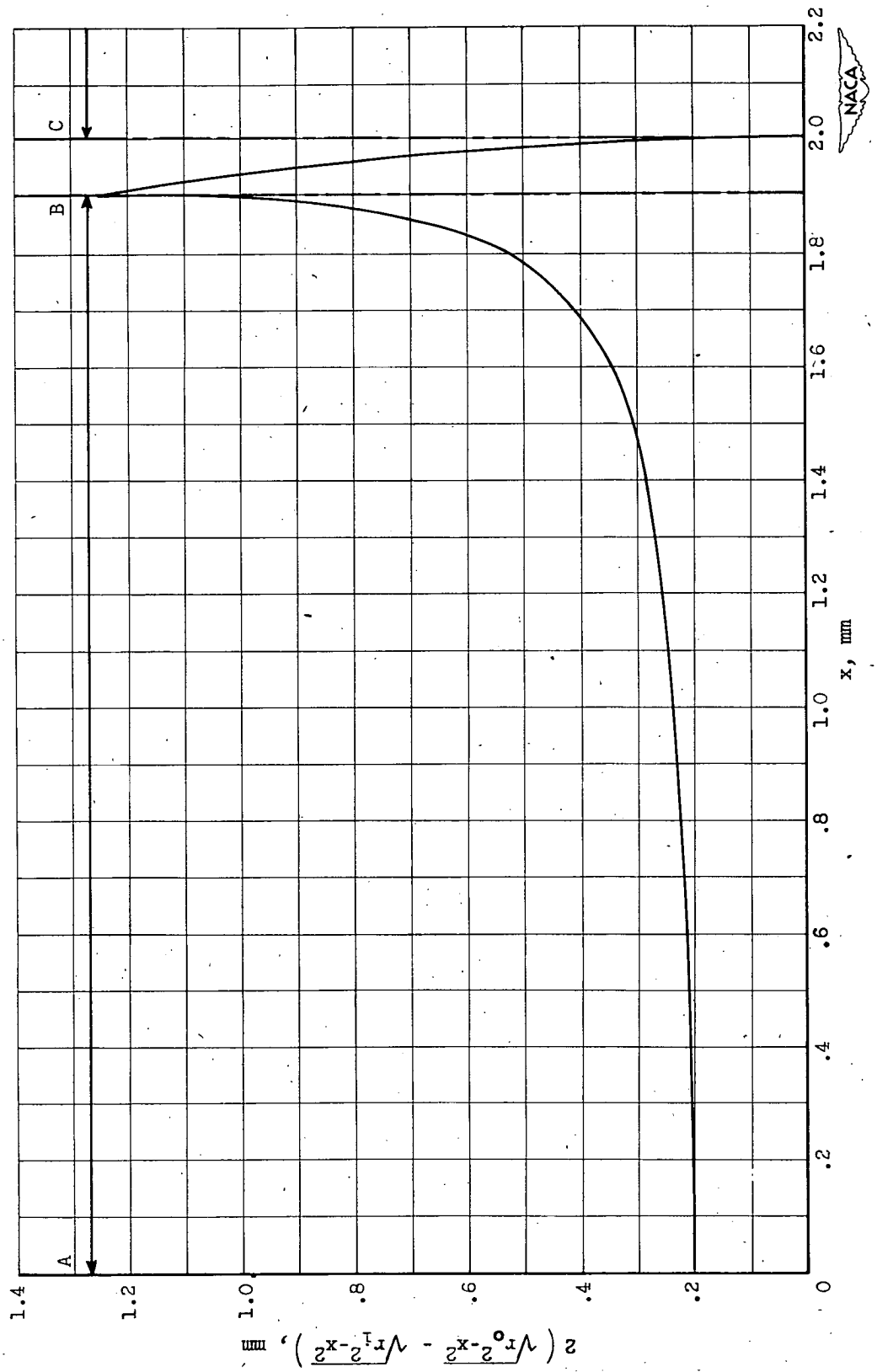

Figure 4. - Variation of ring thickness from center to edge of luminous ring. r_o, 2.0 millimeters; $(r_o - r_i)$, 0.1 millimeter.

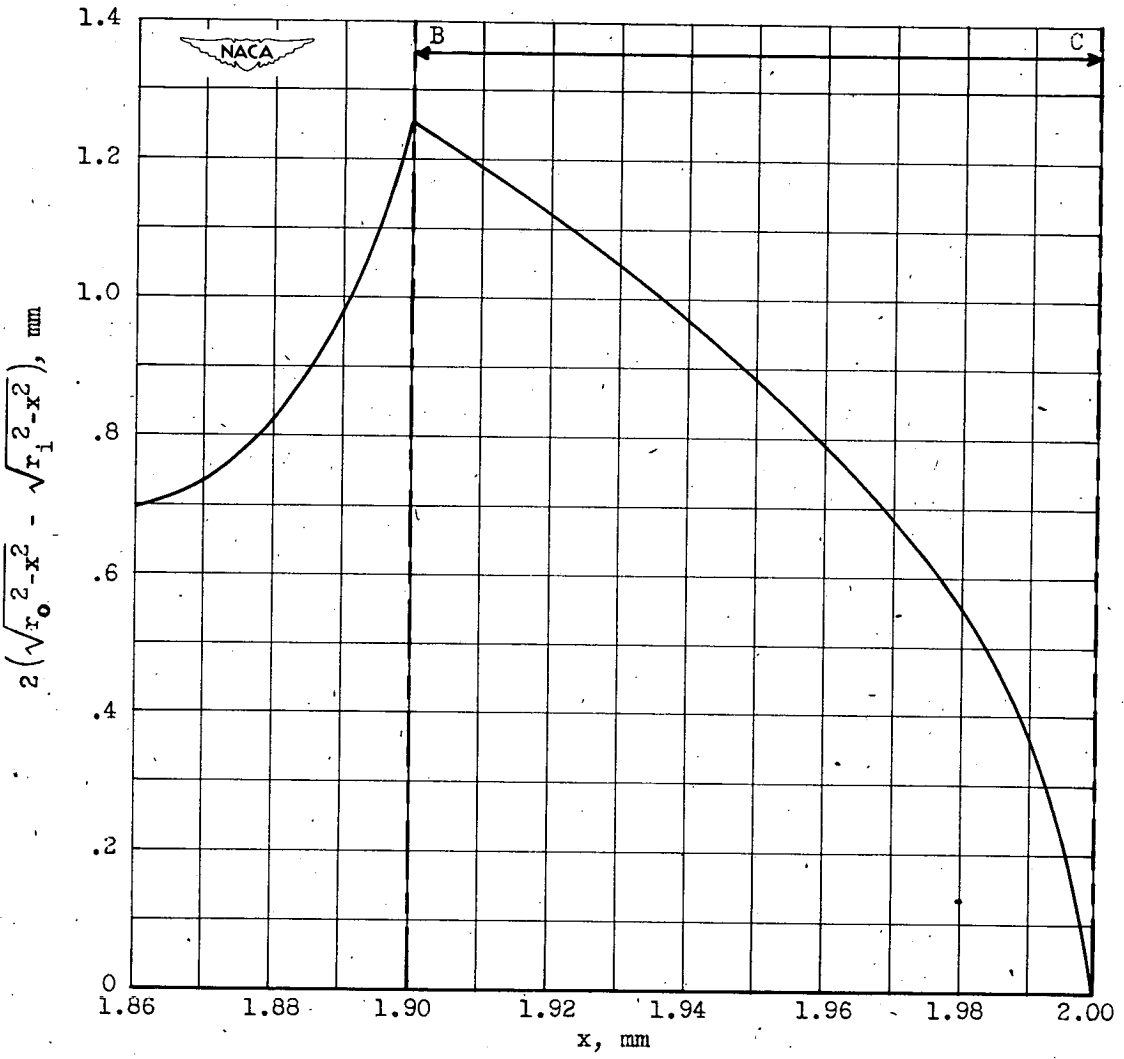

Figure 5. - Variation of ring thickness with distance; horizontal scale X10.

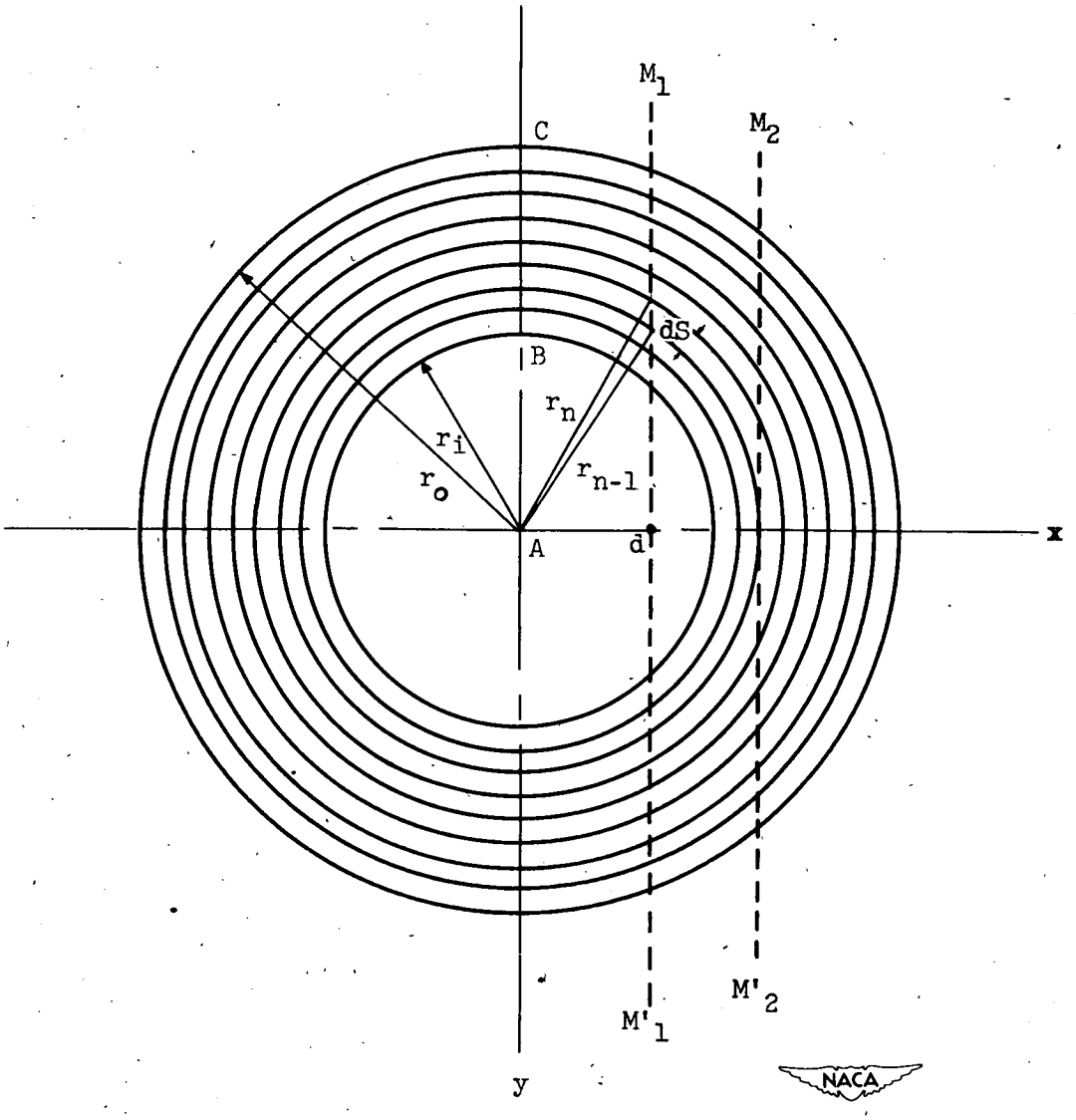

Figure 6. - Diagram of incremental method of determining ring thickness.

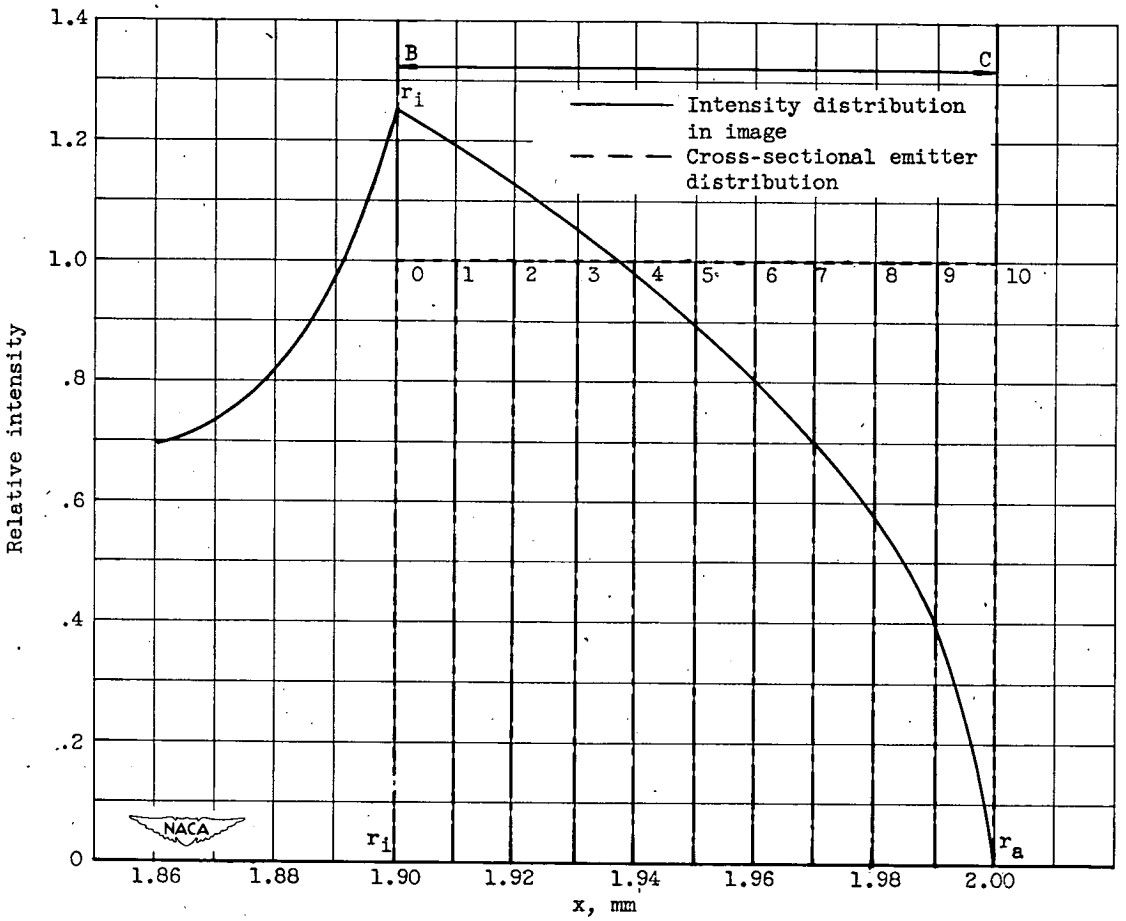

(a) Cross-sectional emitter distribution is of form $y = k$. Equation of cross section, $y = 1$.

Figure 7. - Intensity distribution in ring image.

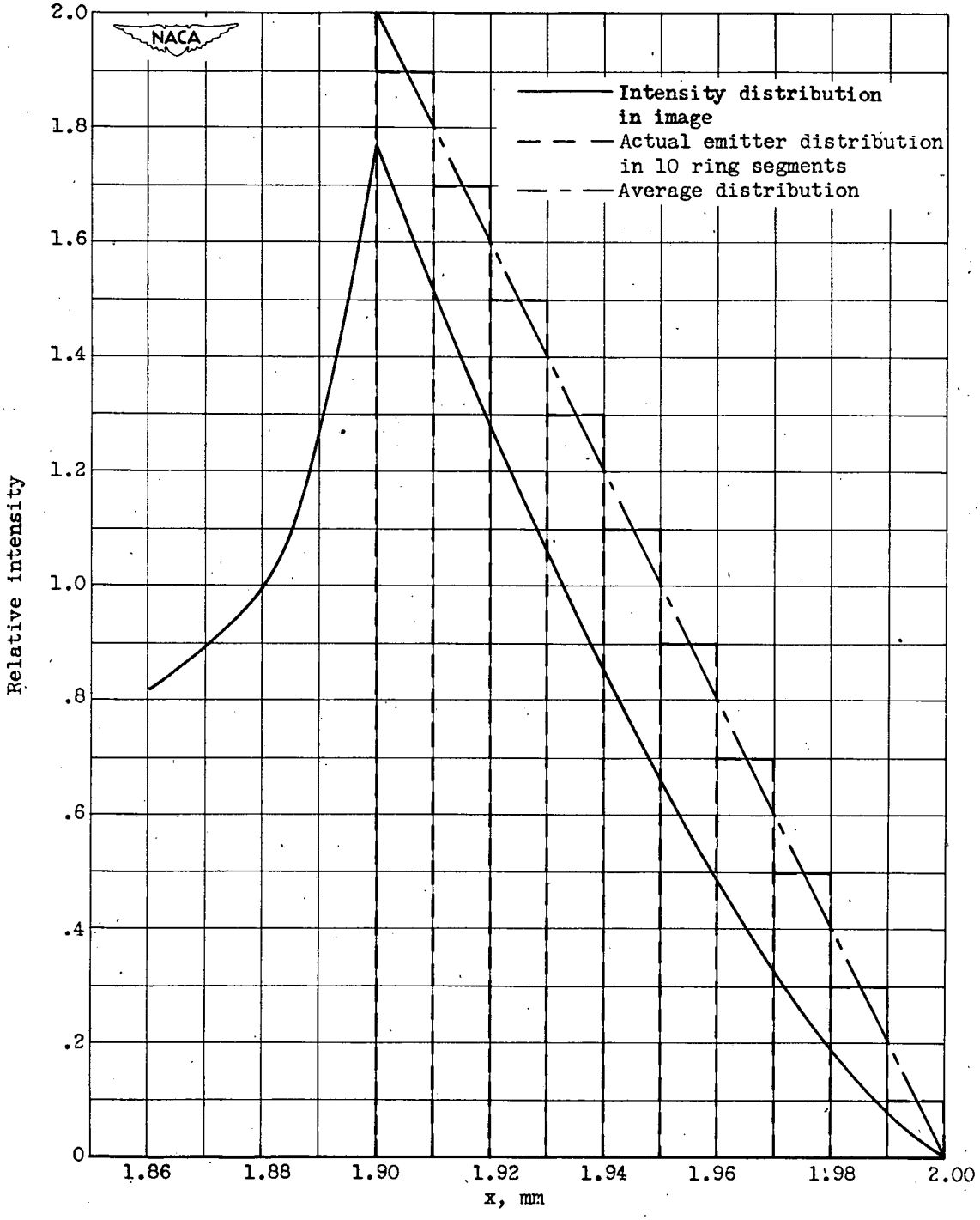

(b) Cross-sectional emitter distribution is of form $y = -kx$.

Figure 7. - Continued. Intensity distribution in ring image.

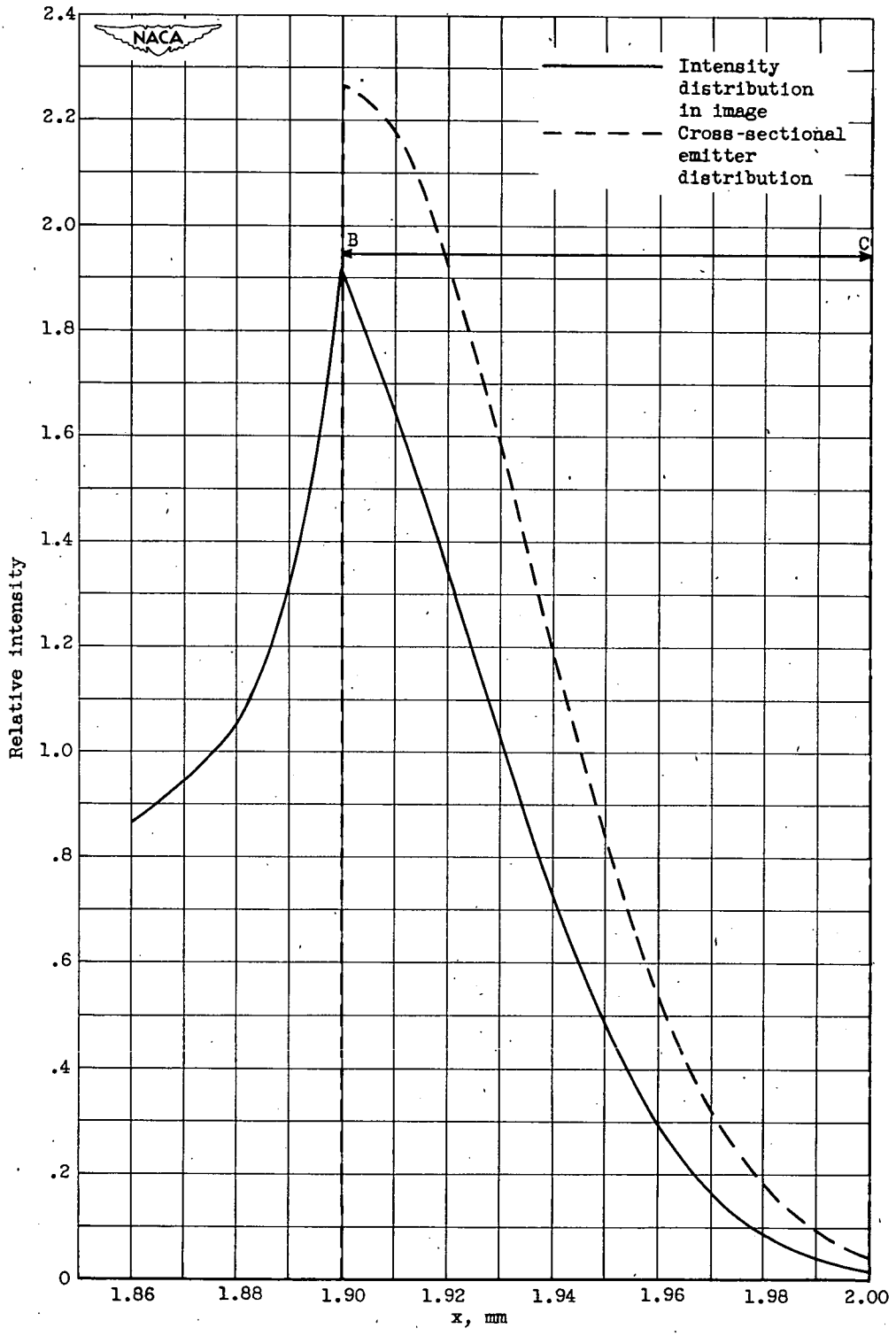

(c) Cross-sectional emitter distribution is of form $y = Ae^{-x^2}$.

Figure 7. - Continued. Intensity distribution in ring image.

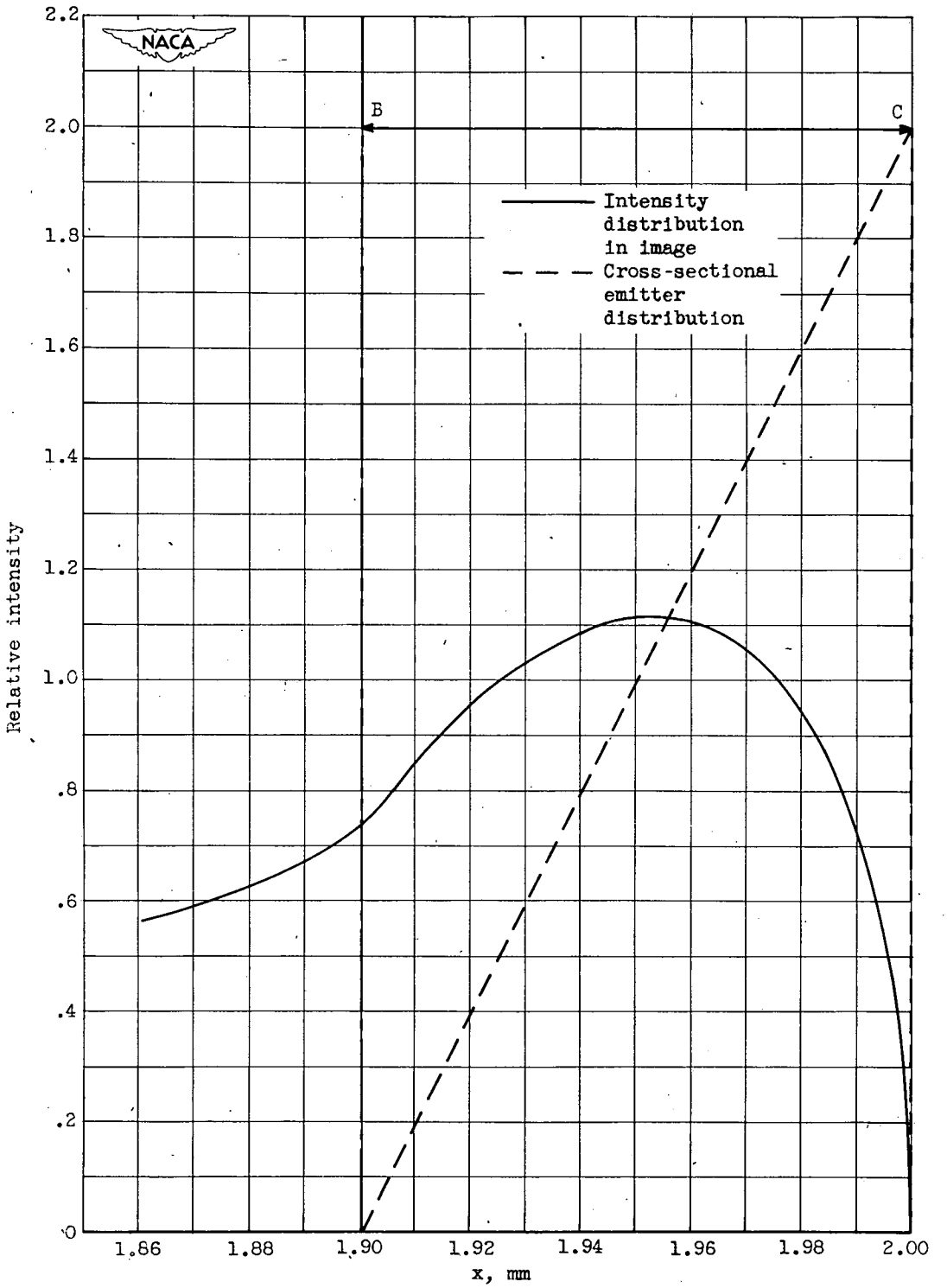

(d) Cross-sectional emitter distribution is of form $y = nx$.

Figure 7. - Continued. Intensity distribution in ring image.

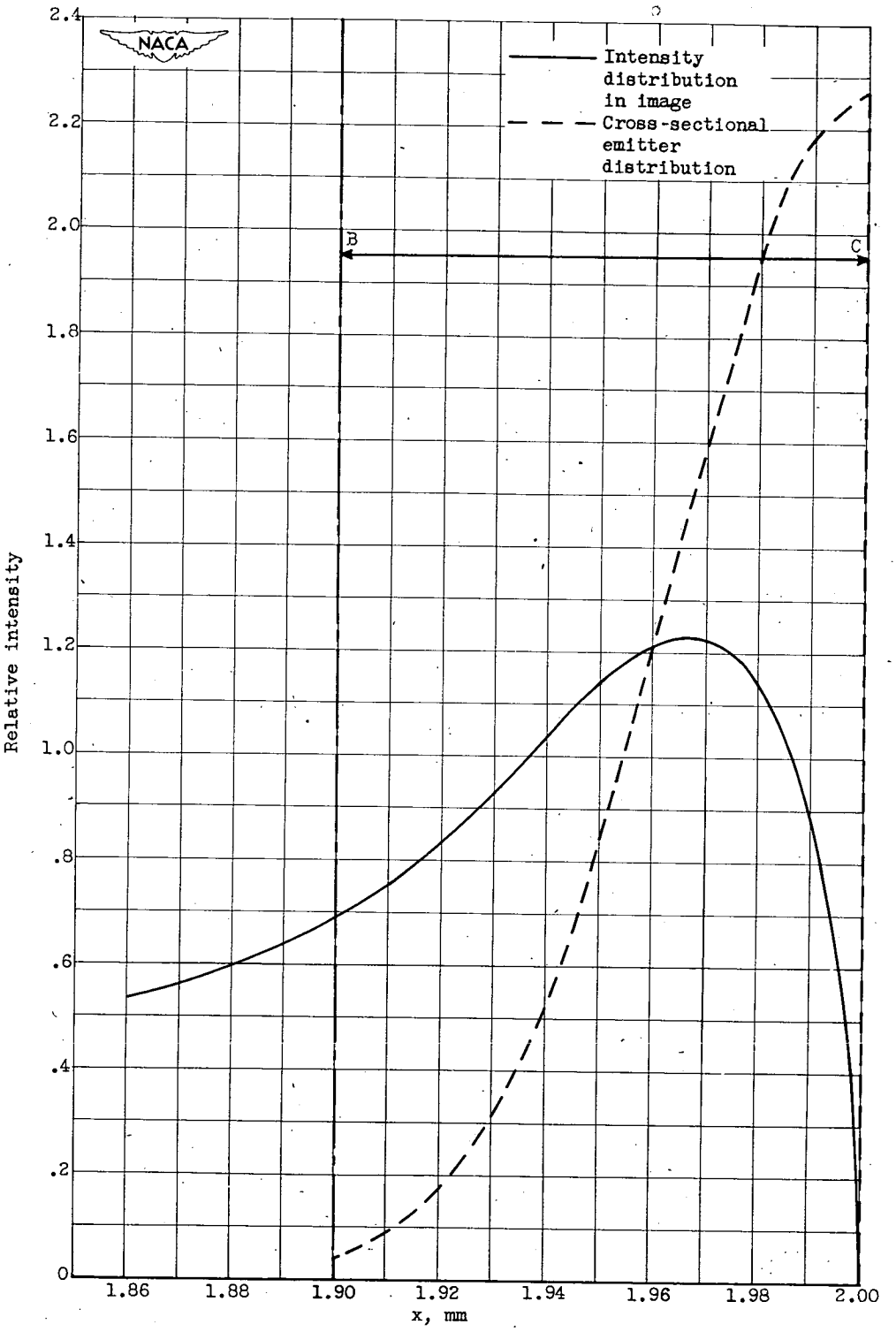

(e) Cross-sectional emitter distribution is mirror image of form $y = Ae^{-x^2}$.

Figure 7. - Continued. Intensity distribution in ring image.

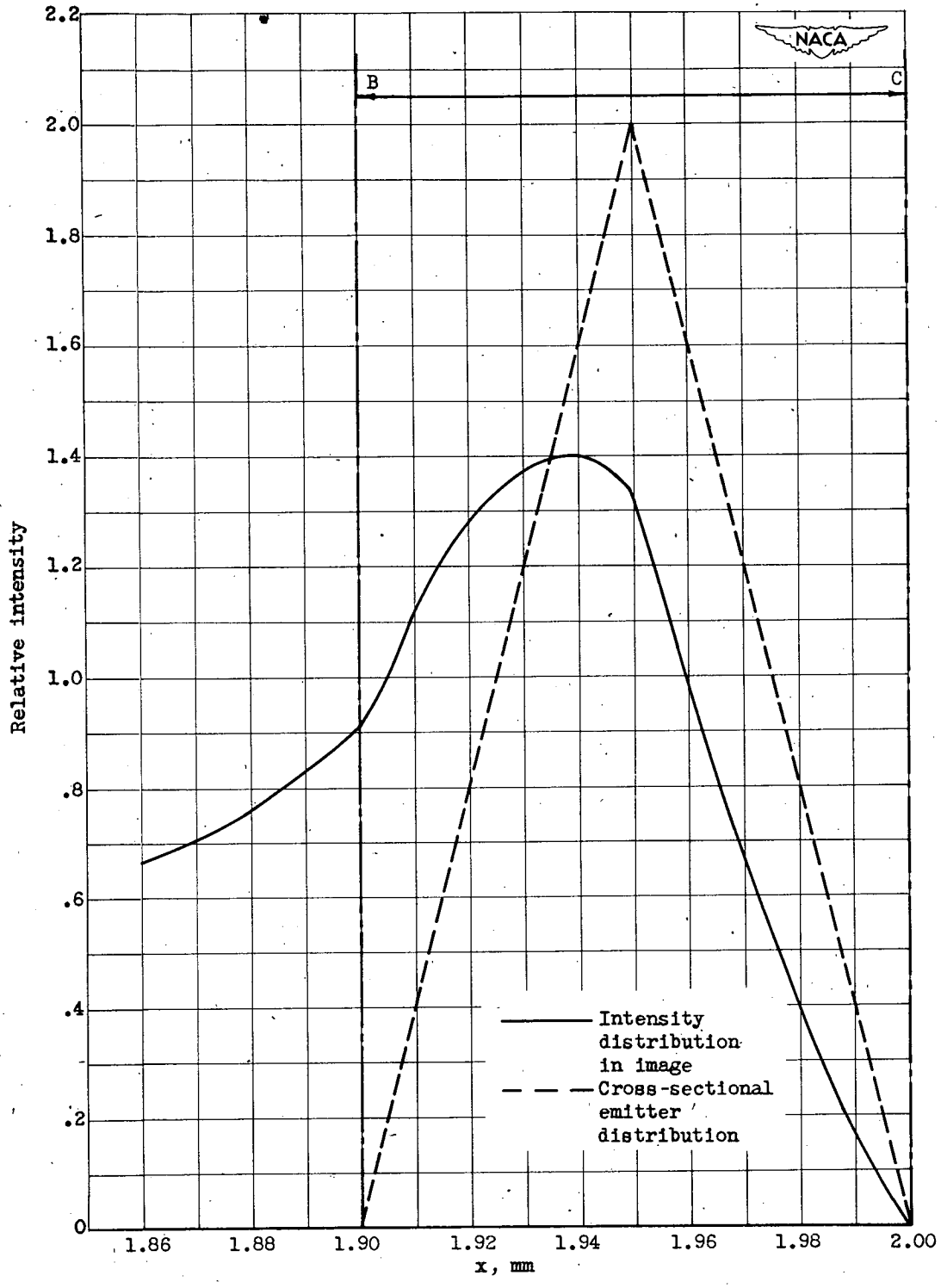

(f) Cross-sectional emitter distribution is of form of straight-sided pyramid.

Figure 7. - Continued. Intensity distribution in ring image.

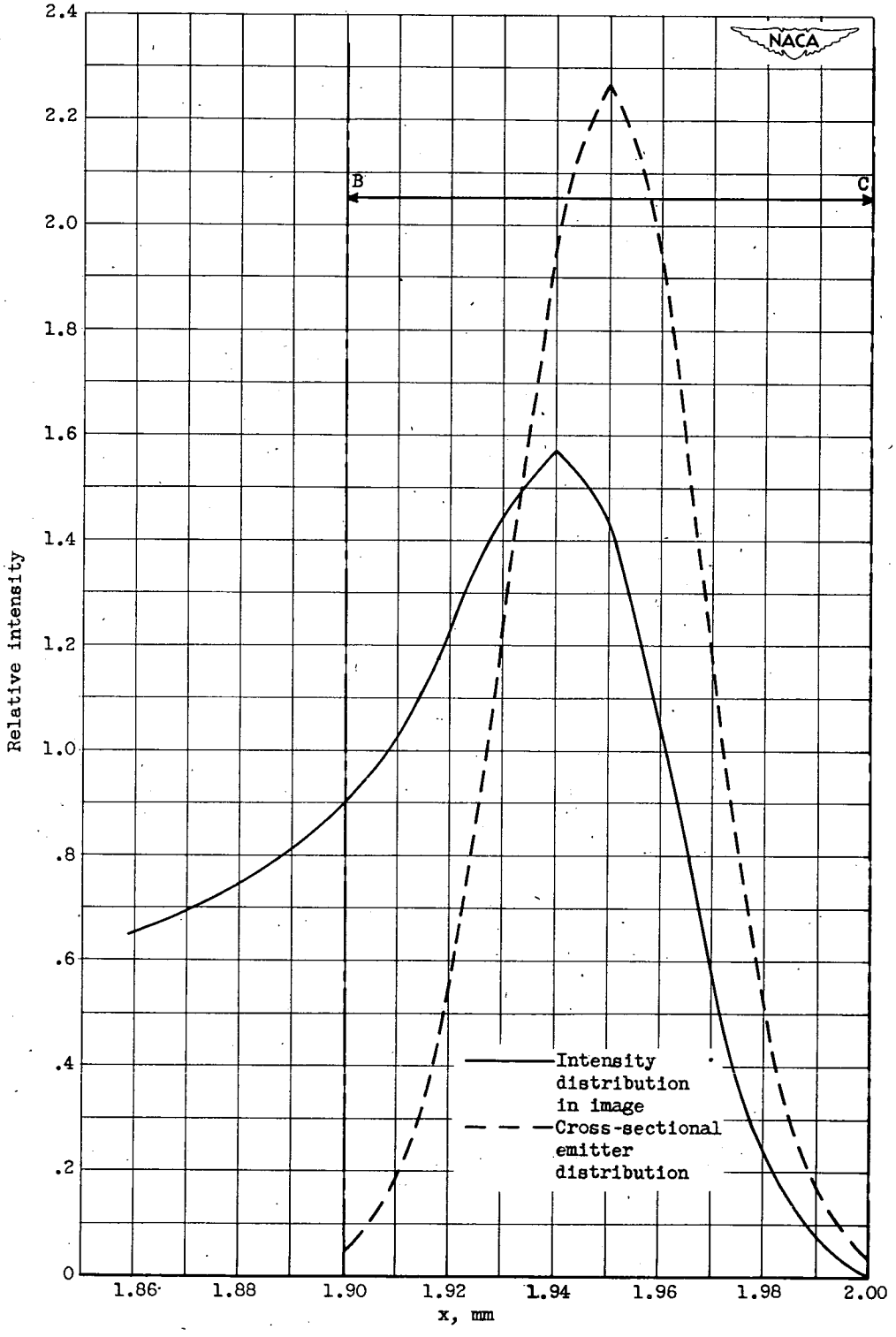

(g) Cross-sectional emitter distribution is of form of Gaussian probability curve $y = Ae^{-x^2}$.

Figure 7. - Concluded. Intensity distribution in ring image.

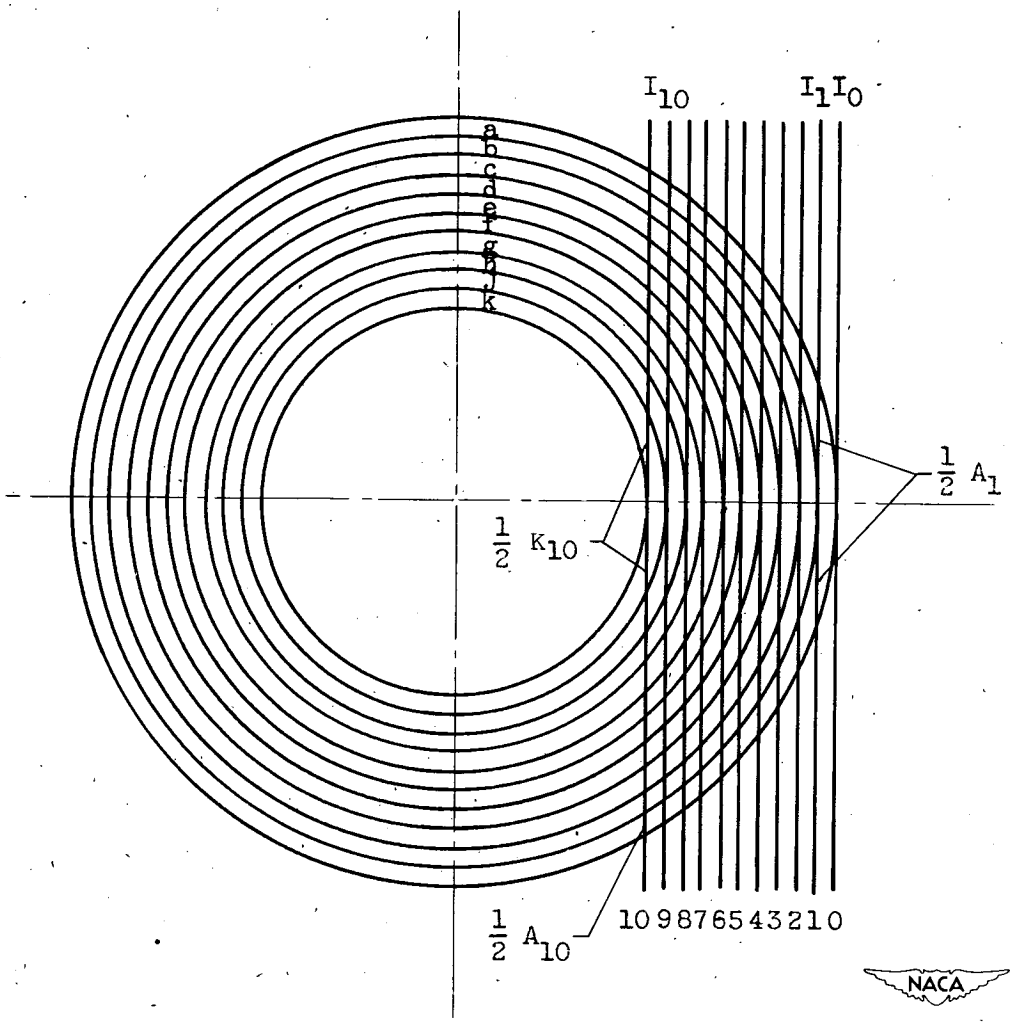

Figure 8. - Diagram of method for calculating emmitter distribution in ring image.

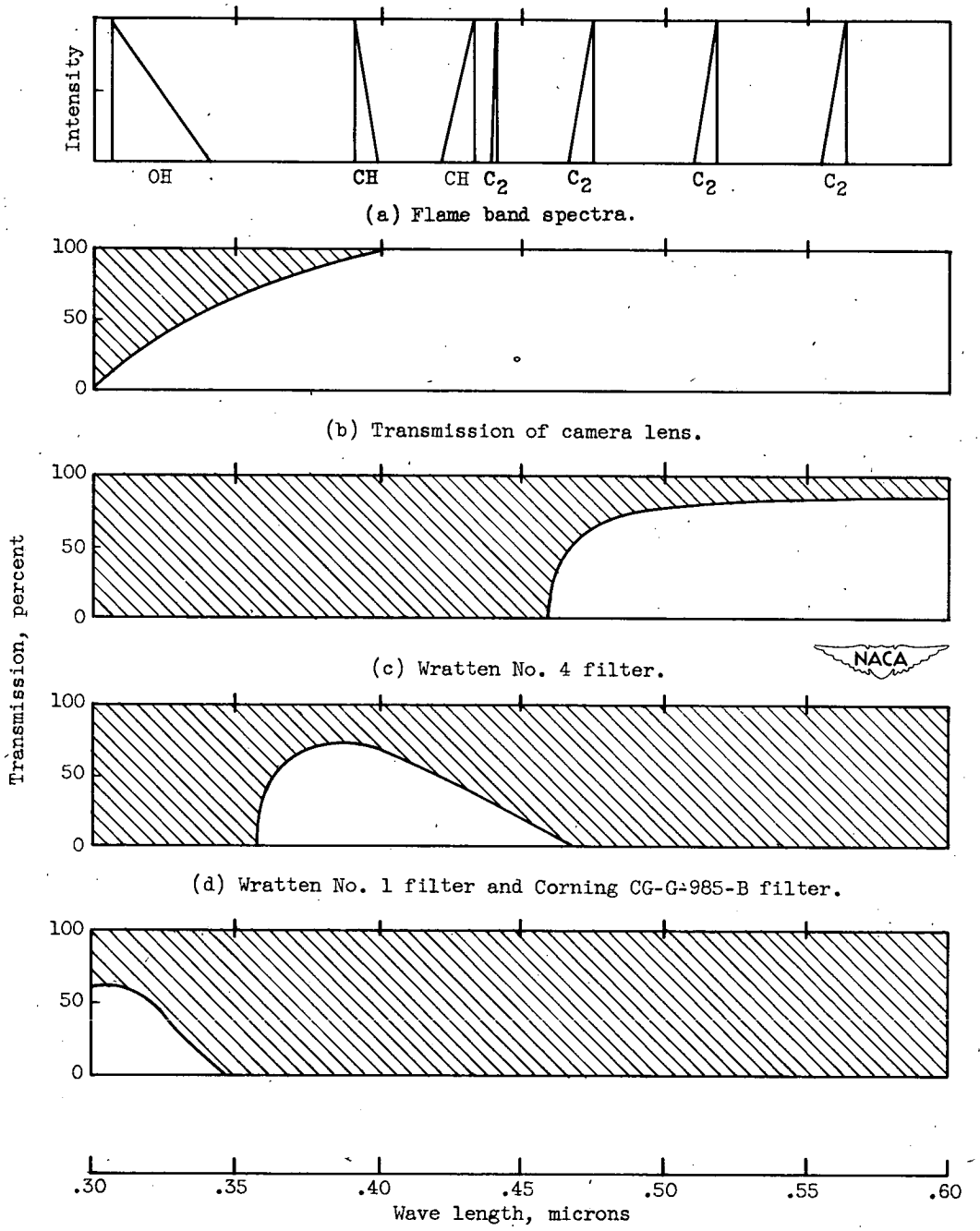

(a) Flame band spectra.

(b) Transmission of camera lens.

(c) Wratten No. 4 filter.

(d) Wratten No. 1 filter and Corning CG-G-985-B filter.

(e) Solution of $NiSO_4$ and $CoSO_4$; thickness, 1 centimeter.

Figure 9. - Transmission characteristics of filters for isolating band spectra in flames. All clear portions indicate light transmission.

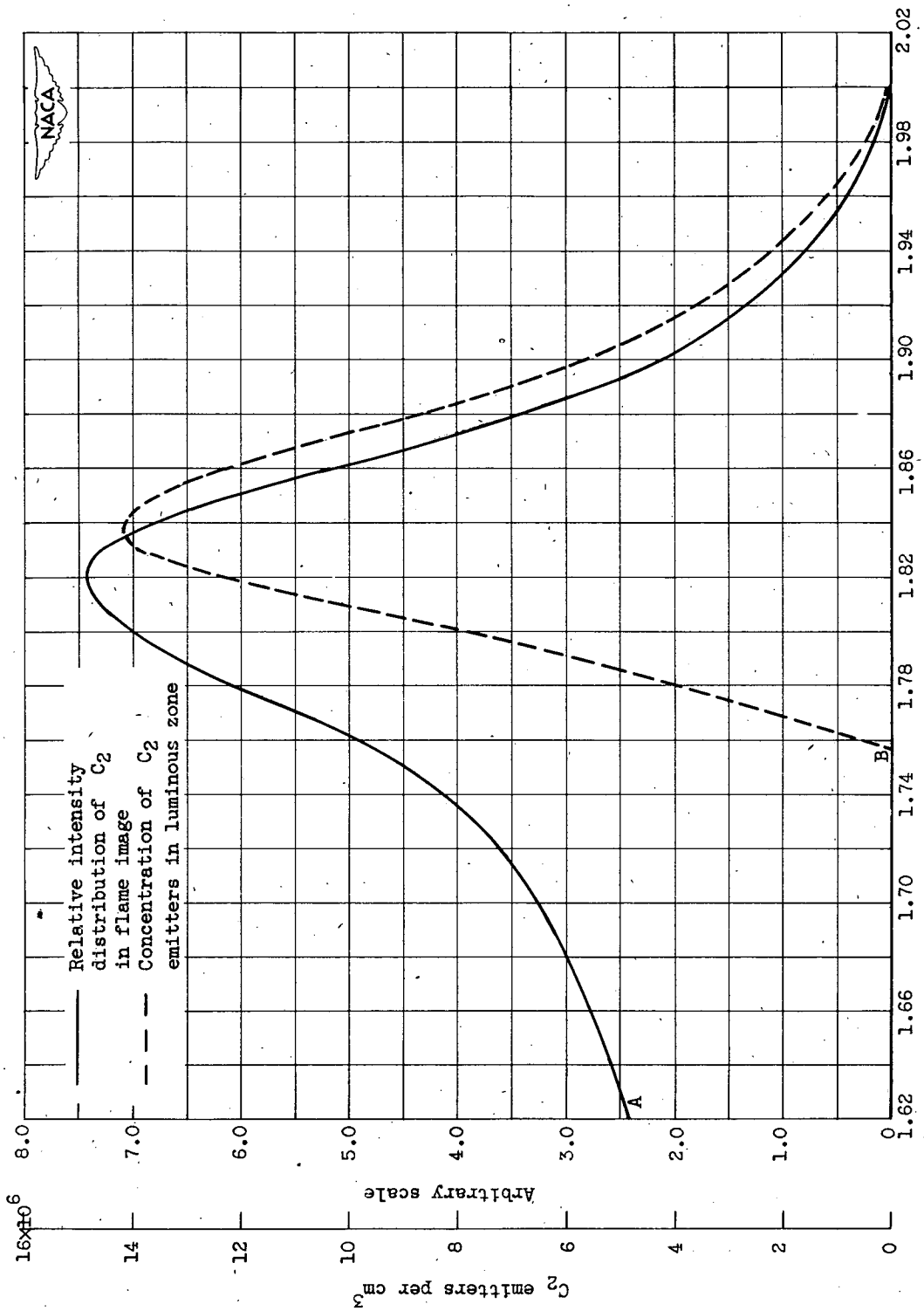

Figure 10. - Intensity distribution and C_2 distribution in flame front of stoichiometric Bunsen flame of propane and air. Volume flow of air, 40 cubic centimeters per second (stoichiometric mixture with propane); dimensions of flame cone: height, 9.0 millimeters; diameter of base, 6.0 millimeters.